EFFECT OF RADIATIVE COOLING ON CLOUD-SST RELATIONSHIP

WITHIN THE TROPICAL PACIFIC REGION

Chung-Hsiung Sui[1], Chang-Hoi Ho[2], Ming-Dah Chou[1], Ka-Ming Lau[1], and Xiaofan Li[1]

[1]NASA/Goddard Space Flight Center, Greenbelt, Maryland, USA

[2]Seoul National University, Seoul, Korea

A recent analysis (*1*) found a negative correlation between the area-mean cloud amount and the corresponding mean SST within the cloudy areas. The SST-cloud relation becomes more evident when the SST contrast between warm pool and surrounding cold pool (dSST) in the tropical Pacific is stronger than normal. The above feature is related to the finding that the strength of subsidence over the cold pool is limited by radiative cooling because of its small variability. As a result, the area of radiatively-driven subsidence must expand in response to enhanced low-boundary forcing due to SST warming or enhanced basin-scale dSST. This leads to more cloud free regions and less cloudy regions. The increased ratio of cloud-free areas to cloudy areas leads to more high SST areas (>29.5°C) due to enhanced solar radiation.

Relationship between sea surface temperature (SST) and cloud/water vapor bears important information about radiation-climate feedbacks (*1, 2, 3*). A recent study examined the mean cloudy area in the tropical western Pacific as a function of the corresponding mean SST in cloudy areas (*1*). The study reveals a 15% reduction in cloudy area for a 1°C increase of the cloud-weighted SST. The negative cloud-SST is suggested to lead to a negative feedback in the global climate through enhanced longwave cooling in the dry subsidence regions. In the current study, we show that the area mean cloud-SST relation found in (*1*) is most evident when the SST contrast between the warm pool and the surrounding ocean is stronger than normal. This is interpreted as a regulation of clouds over the Pacific warm pool by atmospheric radiative cooling in the subsidence region surrounding the warm pool.

First, we examine the SST-convection relationship in the tropical deep convective regime and the surrounding subsidence regime in a cumulus ensemble model (*4, 5*). The model is constrained by an imposed warm-pool and cold-pool SST contrast ($dSST \equiv SST_{w.pool} - SST_{c.pool}$). The domain-mean vertical motion is also constrained to provide a heat sink and moisture source in the model to emulate the observed tropical climate condition. In three experiments, the warm pool SST is specified at 28.5, 29.5, and 30.5°C while the cold pool SST is specified at 26°C (referred to as R, R1, and R2, respectively). The corresponding dSST of the three experiments are respectively, 2.5, 3.5, and 4.5°C. A circulation with mean ascending (descending) motion over the warm (cold) pool is developed in all experiments. The strength of the circulation increases from R to R1 when $dSST \leq 3.5$ °C, and remains unchanged from R1 to R2 when dSST exceeds 3.5°C. This can be explained by the change in heat budget in the subsidence regime where radiative cooling changes little. In weak low-boundary forcing condition ($dSST \leq 3.5$°C), an enhanced subsidence warming in response to a

2

perturbed SST forcing is balanced by a reduced condensation heating. In strong low-boundary forcing condition (dSST>3.5°C), the subsidence regime becomes too stable for condensation heating to occur so that a further enhanced subsidence warming can no longer be sustained. As a result, the area of subsidence increases in response to an increased low-boundary forcing. The overall circulation responses to SST forcing in the strong and weak low-boundary forcing conditions are summarized in Fig. 1.

The change of cloud amount and rain in the above experiments are shown in Table 1. The averaged cloud amount over the total domain increases by 3% from R to R1 (dSST<3.5°C). However, total cloud amount decreases slightly (-0.1) from R1 to R2 when dSST>3.5°C. This shows the change of cloud amount with increasing SST depends on the change of SST-induced internal circulation that is regulated by radiative cooling in the subsiding atmosphere. A further examination of the cloud amount over warm pool shows an increase of 1.1% from R to R1, but a decrease of 0.7% from R1 to R2. The latter is related to the increased area of subsidence (figure not shown). Because radiative cooling in cloud-free regions limits the strength of subsidence as discuss above, the only way to adjust to the enhanced low-level pressure gradient by dSST is to have near-uniform downward motion in a broader area and stronger upward motion in a smaller area to maintain mass balance. The mean rainfall over the warm pool indeed increases 1.4 mm day^{-1} from R1 to R2.

Because all experiments are constrained by the same domain-mean vertical motion, the change of clouds over the cold pool is expected to be opposite to that over the warm pool, i.e. decreased clouds in R1-R and increased clouds in R2-R1. However, the cloud change over the cold pool in R1-R actually increase by 1.9% although area-mean rainfall over the warm pool and cold pool are of opposite signs. This is related to the change of passive clouds (non-

3

raining stratiform clouds in the model). Since passive clouds consist of high clouds (above 500 hPa) originated from deep convective clouds, the change of passive clouds is not only regulated by circulation in the cold pool but also related to the change of convective clouds over the warm pool. We note the change of passive clouds in the cold pool may subject to model limitations including 2-D and an insufficient domain size.

Table 1 Change of cloud amount (percent of area) and rain (mm day^{-1})

	Warm pool Cloud rain	Cold pool Cloud rain	Total domain Cloud
R1-R	1.1 5.0	1.9 -2.2	3.0
R2-R1	-0.7 1.4	0.7 0	-0.1

Next, we seek supporting evidence for the above model results by analyzing high cloud amount (A_{HC}) and vertical p-velocity (ω) (6, 7) as a function of SST (8). The tropical Pacific within 20°S-20°N, 130°E-110°W is chosen as our analysis domain. Within it, warm pool and cold pool are separated by an isotherm so determined that the area of warm pool is 25% of the analysis domain. There exists a strong negative relation between cold pool SST and dSST ($SST_{w.pool}$ - $SST_{c.pool}$) due to the El Nino -Southern Oscillation (ENSO) evolution, and a weak positive relationship between warm pool SST and dSST due to the significant contribution by seasonal cycle in addition to the ENSO evolution.

Mean A_{HC} over the warm pool and cold pool as a function of dSST is shown in Fig. 2a. A_{HC} over the warm (cold) pool appears to be positively (negatively) correlated with dSST for dSST<2.6°C. This correlation is consistent with the increased ascending (descending) motion over the warm (cold) pool associated with enhanced dSST as shown by the $-\omega$ at 500 hPa level in Fig. 2b. The correlation is reversed for dSST>2.6°C, consistent with the model

4

results discussed above. Note that the different threshold of dSST between the model results and observations is primarily due to the different area ratio between warm pool and cold pool. In comparison of the above analysis with model results, we note that, unlike the model experiments, the mean vertical motion in the domain of analysis varies and is expected to influence the SST-cloud/water vapor relationship. To further clarify the results, A_{HC} and ω in Fig.2 are shown in three categories of ω at 500 hPa: $(\omega-\omega_m)<-2$ mbday^{-1} (red), $|\omega-\omega_m|<2$ mbday^{-1} (green), and $(\omega-\omega_m)>2$ mbday^{-1} (blue), where ω_m is the time mean ω. The circulation-stratified A_{HC} as a function of dSST shows several important features. First, A_{HC} is generally highest in category 1 and lowest in category 3. Second, A_{HC}-dSST relationship discussed above is more evident in each category. Since cloud and water vapor are closely related, we also examined the relationship between vertically integrated water vapor, PW, and SST. Since A_{HC} and PW are positively correlated, PW-dSST relationship is similar to the A_{HC}-dSST relationship except for weak dSST($<2.3°$C). For brevity, the results are not shown here. The overall observational evidence is consistent with model results.

In the following, we show evidence that the above mechanism regulates the negative relationship between cloudy area as measured by the Japanese GMS-5 geostationary satellite, and the mean SST within the cloudy areas (1). We examined the area mean A_{HC} over the domain (20°S-20°N, 130°E-110°W) as a function of mean SST within cloudy areas, and found a similar negative cloud-SST relationship as found by (1). Furthermore, the A_{HC}-SST relation is examined in stronger dSST ($>2.6°$C) and weaker dSST ($<2.3°$C) categories (Fig. 3). The results show that the negative relationship is most evident in the stronger than normal dSST category. Figure 3 and Fig. 2 together support the model results that show the regulation of SST-cloud relation by radiative cooling (Table 1).

5

Finally, the area mean SST-cloud relation and its regulation can be considered in a different perspective by examining the grid values of A_{HC} as a function of SST for the stronger dSST (>2.7°C) category and the weaker dSST (<2.2°C) category over the tropical Pacific domain (Fig. 4). Also shown in Fig. 4 are the SST histograms in the two dSST categories that reveal less warm SST areas (27°C<SST<29.5°C) and more cold SST (SST<27°C) areas in the stronger dSST category than in the weaker dSST category. The former is representative of the La Nina situation. Despite the differences in SST histograms, the figure reveals some common features in the two dSST categories: 1) most clouds occur over warm pool (SST>28°C), and they tend to increase with increasing SST up to 29°C, 2) high SST areas (>29°C) decrease rapidly. These features are consistent with previous findings (9, 10, 11, 12, 13). Note, however, that mean cloud amounts over cold SST (SST<27°C) are generally lower in the stronger dSST category than in the weaker dSST category, suggesting a regulation effect by radiative cooling over cold SSTs in the stronger dSST category. For SST>29°C, SST-cloud correlation shows a tendency to change from positive to negative, and this tendency is more evident in the stronger than normal dSST category. This is consistent with previous analysis that the cloud-free area is larger and the cloudy area is smaller in stronger than normal dSST. The larger cloud-free area leads to more high SST areas due to enhanced solar radiation as shown by the SST histogram shown in Fig. 4.

In the analysis of SST-cloud relationship, scale dependence must be considered. An important factor in the analysis of (1) is the size of the domain. We carried out an analysis (14) that shows that a stable negative cloud-SST relation found in (1) cannot be realized without considering the entire tropical Pacific basin. Another concern is the intraseasonal

variability that may affect the observed cloud-SST correlation as suggested in recent analysis of TOGA COARE data (*15, 16*). We note that the intraseasonal variability is excluded in the analysis of (*10*).

The negative correlation between cloud amount and SST appears to be a fundamental relation that needs to be explained. One is attributed by (*1*) to microphysics, i.e. coalescence proceeds more rapidly with increasing air temperature (linked to SST) and results in a reduced cirrus outflow. In this reasoning, cloud changes as a response to SST changes. An opposite interpretation of the negative SST-cloud relation shown in Fig. 4 is offered by (*10, 3, 11*) that related SST changes as a response to cloud changes. The current analysis indicates a regulation effect of the SST-cloud relation by radiative cooling in cloud-free regions. In studying the cloud-radiation-SST problem, one must consider coupled ocean-atmosphere dynamic processes that maintain the tropical climate system (17, 18).

REFERENCES AND NOTES

(1) Lindzen, R. S., M.-D. Chou, A. Hou, 2000: Does the earth have an adaptive infrared iris? Submitted to *Bull. Am. Meteorol. Soc*

(2) Lindzen, R. S., 1990: Some coolness concerning global warming. *Bull. Amer. Meteor. Soc.*, **71**, 288-299.

(3) Ramanathan, V., and W. Collins, 1991: Thermodynamic regulation of ocean warming by cirrus clouds deduced from observations of the 1987 El Nino. Nature, 351, 27-32.

(4) Tao, W.-K., and J. Simpson, 1993: The Goddard Cumulus Ensemble Model. Part 1: Model description. *Terrestrial, Atmospheric and Oceanic Science*, **4**, 35-72.

(5)   Sui, C.-H., K.-M. Lau, W.-K. Tao and J. Simpson, 1994: The tropical water and energy cycles in a cumulus ensemble model. Part 1: Equilibrium climate. *J. Atmos. Sci.* **51**, 711-728, 1994.

(6)   Rossow, W. B., and R. A. Schiffer, 1991: ISCCP Cloud Data Products. *Bull. Am. Meteorol. Soc.,* **72**, 2-20. ISCCP D1 data are averaged to 2.5°x2.5° longitude-latitude spatial resolution and monthly time scale for the period of July 1983 - August 1994. The high cloud amount (A_{HC}) is defined to be the fractional area within each grid by clouds at levels higher than 440 hPa.

(7)   Kalnay, E., and Coauthors, 1996: The NMC/NCAR 40 year reanalysis project. *Bull. Am. Meteorol. Soc.,* **77**, 437-471. The NCEP/NCAR has a horizontal resolution of 2.5°x2.5° longitude-latitude and available for 1949-1999 at present.

(8)   Reynolds, R. W., and T. S. Smith, 1994: Improved global sea surface temperature analysis. *J. Climate.* **7**, 929-948. SST data is available on a T62 Gaussian grid (~1.87°x1.87° longitude-latitude). To be consistent with ISCCP high cloud amount, SST is degraded to 2.5°x2.5° longitude-latitude by linear interpolation.

(9)   Gadgil, S., P. V. Joseph, and N. V, Joshi, 1984: Ocean-atmospheric coupling over monsoon regions. *Nature,* **312**, 141-143.

(10)   Graham, N., and T. P. Barnett, 1987: Sea surface temperature, surface wind divergence, and convection over tropical oceans. *Science,* **238**, 657-659.

(11)   Waliser, E. E., and N. E. Graham, 1993, Convective cloud systems and warm-pool SSTs: Coupled interactions and self-regulation. J. Geophys. Res, 98(D7), 12881-12893.

(12) Lau, L.-M., H-T. Wu, S. bony, 1997: The role of large-scale atmospheric circulation in the relationship between tropical convection and sea surface temperature. *J. Climate*, **10**, 381-392.

(13) Waliser, D. E., 1996: Formation and limiting mechanisms for very high sea surface temperature: Linking the dynamics and thermodyanmics. *J. Climate*, **9**, 161-188.

(14) Ho, C.-H., C.-H. Sui, and M.-D. Chou, 2000: A regulation of high cloud over tropical Pacific ocean.

(15) Sui, C.-H., X. Li, K.-M. Lau, and D. Adamec, 1997: Multi-scale air-sea interaction during TOGA COARE. *Mon. Wea. Rev.* **125**, 448-462.

(16) Lau, K.-M., and C.-H Sui, 1997: Mechanisms of short-term sea surface temperature regulation: observations during TOGA COARE. *J. Climate*, **10**, 465-472.

(17) Liu, Z., and B. Huang, 1997: A coupled theory of tropical climatology: warm pool, cold tongue, and Walker circulation. *J. Climate*, **10**, 1662-1679.

(18) Jin, F.-F., 1996: Tropical ocean-atmosphere interaction, the Pacific cold tongue, and the El Nino-Southern oscillation. *Science*, **274**, 76-78.
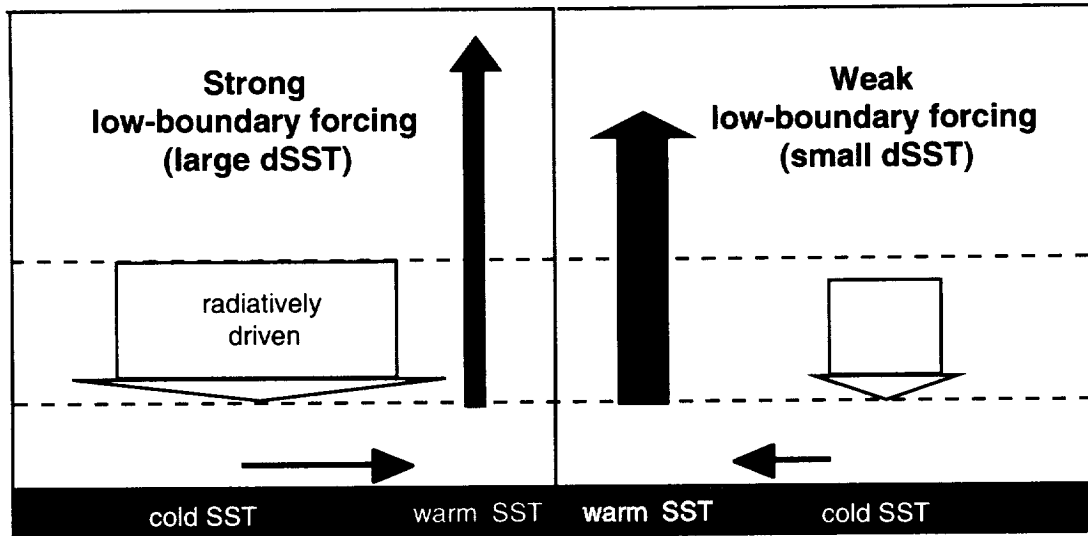
Fig. 1 Schematic summary of responses of tropical circulation (V and w by horizontal and vertical arrows) to perturbed SST forcing in strong & weak low-boundary forcing regimes. The area and strength of V and w are proportional to the width and length of the arrows, respectively.

(a)   (b)
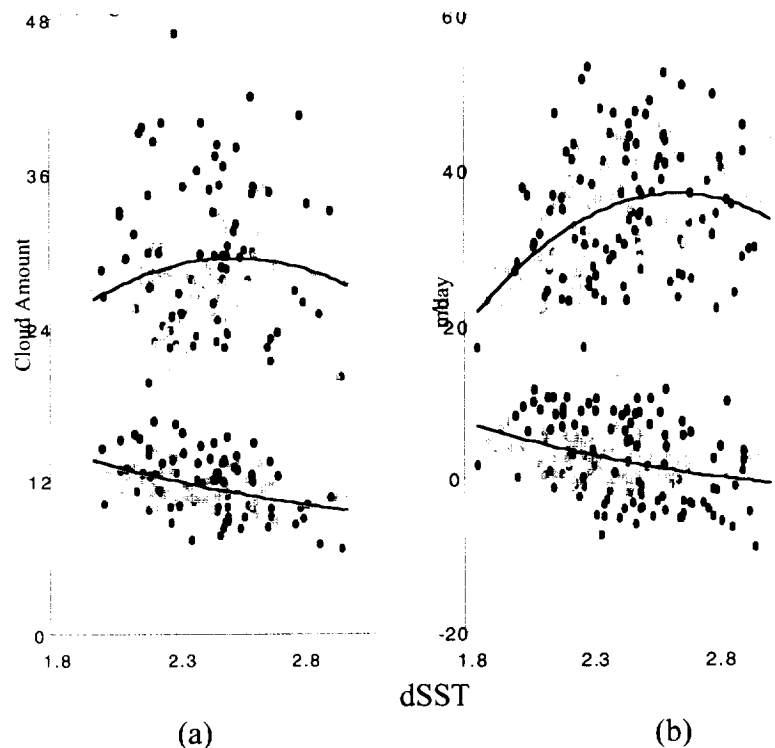
Fig.2 Scatter plot of A_{HC} (a), and $-\omega(500\ hPa)(b)$ over the warm pool (upper) and cold pool (lower) as a function of dSST. Red, green, and blue dots correspond to the three categories of ω

10
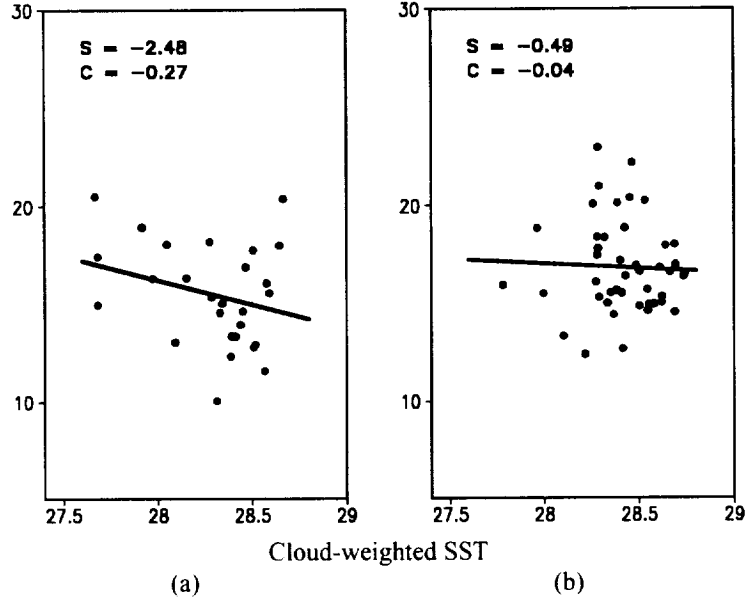
Fig. 3 Scatter plot between area mean SST and cloud weighted A_{HC} in the tropical Pacific (20°S-20°N, 130°E-110°W) for (a) dSST>2.6°C, and (b) dSST<2.3°C.
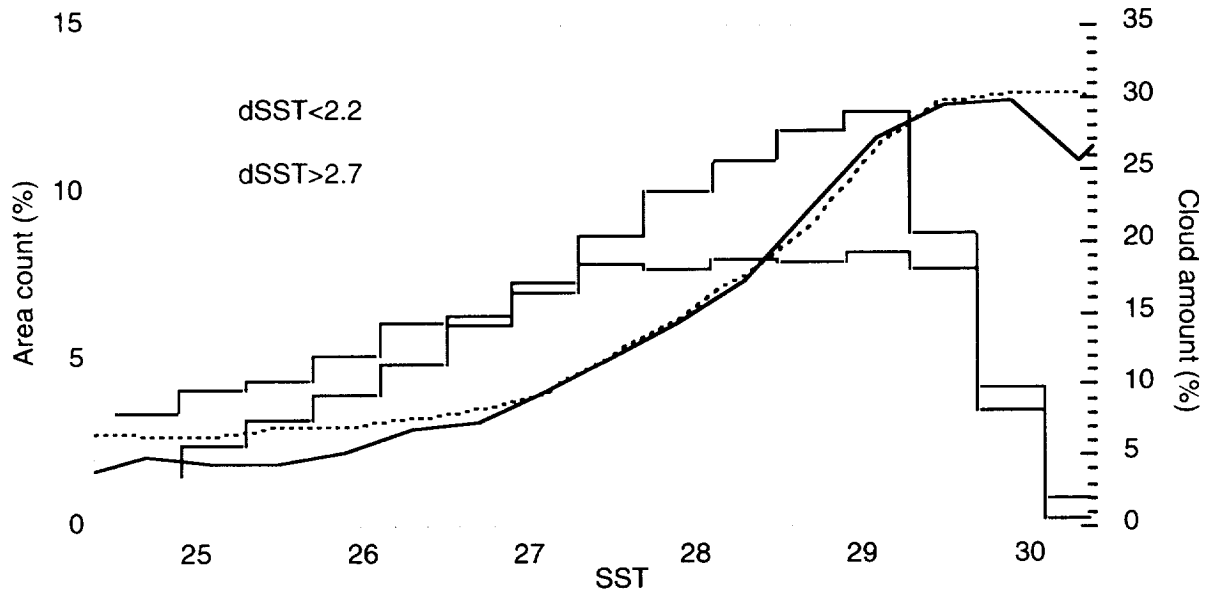
Fig. 4 Relationship between collocated SST and A_{HC} in the tropical Pacific (20°S-20°N, 130°E-110°W) for dSST>2.7°C, and dSST<2.2°C, expressed as the mean A_{HC} values within every 0.4°C SST bin. Vertical bars indicate standard deviation of A_{HC} from the mean value within each SST bin. The corresponding histograms of SST are also shown in terms of fractional area.